STANDING WAVE PATTERNS AT LIQUID NITROGEN CALIBRATION OF MICROWAVE RADIOMETERS

Bernhard Pospichal[1], Gerrit Maschwitz[2], Nils Küchler[2], and Thomas Rose[3]

[1]*University of Leipzig, Stephanstr. 3, 04105 Leipzig, Germany, email: bernhard.pospichal@uni-leipzig.de*
[2]*University of Cologne, Zülpicher Str. 49a, 50674 Köln, Germany*
[3]*Radiometer Physics GmbH, Birkenmaarstr. 10, 53340 Meckenheim, Germany*

ABSTRACT

A standard method for the absolute calibration of passive microwave radiometers is the hot-cold-calibration where two blackbody calibration targets with different physical temperatures are used.

Usually, a liquid nitrogen (LN_2) target with a well-known boiling temperature provides the cold calibration point. In the standard calibration procedure for a ground-based passive microwave radiometer (HATPRO), the integration time on each target is 30–60 seconds.

However, when observing the cold target for a longer time, an oscillation of the incoming power signal with a period of 2–20 minutes is detected. This period is linearly correlated with the microwave wavelength indicating a standing wave between the receiver and the LN_2 surface.

The amplitude of this oscillation corresponds to a brightness temperature range of up to 1.5 K which can lead to an error in the retrieved integrated water vapor of up to 1 kgm^{-2}.

In order to consider this effect it is necessary to integrate over one whole oscillation cycle and taking the mean value as the reference power which corresponds to the boiling temperature of liquid nitrogen.

1. INTRODUCTION

Ground-based passive microwave radiometers are increasingly used for continuous observation of the atmospheric state. These instruments measure radiation emitted by atmospheric components (mainly oxygen, water vapor and cloud liquid). Depending on the frequency bands used, information on temperature profiles, water vapor, and cloud liquid water is provided. Usually, these instruments measure at several frequencies in the K-Band along the 22.235 GHz water vapor absorption line as well as in the V-Band on the lower flank of the 60 GHz oxygen absorption complex [1]. The observed radiation is expressed as blackbody-equivalent brightness temperature. To obtain atmospheric quantities, the application of retrieval algorithms is necessary.

Nowadays, these instruments are designed for continuous and unattended operation. However, the accuracy of the accurate calibration of the radiometer system remains crucial, like for all remote sensing methods. The theoretical error for the retrieved quantities is less than 1 K for temperature profiles in the boundary layer and 2 K above [2]. Integrated water vapor can be obtained better than 0.5 kgm^{-2} and cloud liquid water path with an accuracy of 20 gm^{-2} [3]. In order to reach these values, the brightness temperature accuracy needs to be better than 0.5 K which can only be assured by regular sensor calibration. Ref. [4] give an overview over the HATPRO (Humidity and Temperature Profiler) microwave radiometer which was manufactured by Radiometer Physics GmbH (RPG) and the calibration methods for this instrument.

The present paper will especially focus on the hot-cold calibration of HATPRO radiometers using LN_2. When observing the cold calibration target for a longer time, an oscillation of the incoming power signal with a period of 2–20 minutes was detected. We will examine this feature more deeply in this paper and will estimate the maximum error that may be related.

2. CALIBRATION OF PASSIVE MICROWAVE RADIOMETERS

Calibrating a microwave radiometer means to determine the relationship between the detected voltage at the receiver (U_{det}) and the physical measurement quantity brightness temperature (see Eq. 1, for more details see [5]).

$$U_{det} = g \cdot (T_R + T_A)^\alpha \qquad (1)$$

The receiver input is composed from two sources, T_A being the antenna temperature (represents the incoming power from the atmosphere over the bandwidth of the receiver), and T_R being the system noise temperature. g represents the detector gain and α is a non-linearity factor. For blackbody targets, the physical temperature is equivalent to the antenna temperature which can then be directly inserted to Eq. 1.

At the HATPRO microwave radiometer, several absolute and relative calibration methods are performed (see also [4] and [5]). Before operating HATPRO, the complete set of calibration parameters (α, T_R, g, as well as the noise diode temperature T_N) are determined by a hot-cold absolute calibration. For low-opacity radiometer channels, the so-called tipping curve calibration provides a further absolute calibration standard. Additionally, during operation noise diode calibrations and gain calibrations (hot load) are performed every 30 and 5 minutes, respectively. The latter two methods are relative calibration methods, as not all of the calibration parameters are determined.

3. HOT-COLD CALIBRATION USING LIQUID NITROGEN

For the hot-cold calibration, two targets with well-known and constant, although strongly differing, temperatures are needed. HATPRO's hot target is situated inside the radiometer and consists of a blackbody (styrofoam) load with the temperature T_H. On the outside of the radiometer, another blackbody target is mounted which is being filled with liquid nitrogen so that the temperature T_C corresponds to the boiling point of LN_2 which is around 77 K. After integrating for 30–60 seconds on the hot and cold target, respectively, an additional noise is injected to the system from an internal noise diode T_N. With this set of equations (Eq. 2, the four parameters (α, T_R, g and T_N can be determined.

$$\begin{aligned} U_C &= g \cdot (T_R + T_C)^\alpha \\ U_H &= g \cdot (T_R + T_H)^\alpha \\ U_{CN} &= g \cdot (T_R + T_C + T_N)^\alpha \\ U_{HN} &= g \cdot (T_R + T_H + T_N)^\alpha \end{aligned} \qquad (2)$$

3.1. Uncertainties associated with the LN_2 calibration

There are several known uncertainties with the LN_2 calibration which are listed below, for more details see [5]:

- The reflectivity of the LN_2 surface gives an additional reflective component (1.9 K) that originates from the stabilized receiver (305 K). The reflective component is added to the nominal boiling point. The reflectivity is determined by the refractive index n which is not exactly known ($n = 1.20 \pm 0.03$). At the cold calibration this gives and uncertainty of about 1 K.
- Different manufacturer use different formulation of the pressure-dependent correction of the LN_2 boiling point. TB measurements below in vicinity of the cold calibration point are affected by more than 1 K. However, this uncertainty can be avoided by using the Clausius-Clapeyron Equation.
- The LN_2 calibration is also affected by uncertainties of the hot calibration point. An uncertainty 0.3 K associated with the hot load temperature measurement is estimated from the maximal temperature gradients within the ambient target. Calibrated TB values near the hot calibration are almost fully affected by this uncertainty.

3.2. Oscillating patterns with the LN_2 calibration

When perfoming several LN_2 calibrations directly after each other, the calibration parameters for some channels turned out to differ considerably. Without changing the external conditions and having the cold target still filled with LN_2 completely, the values should not vary strongly.

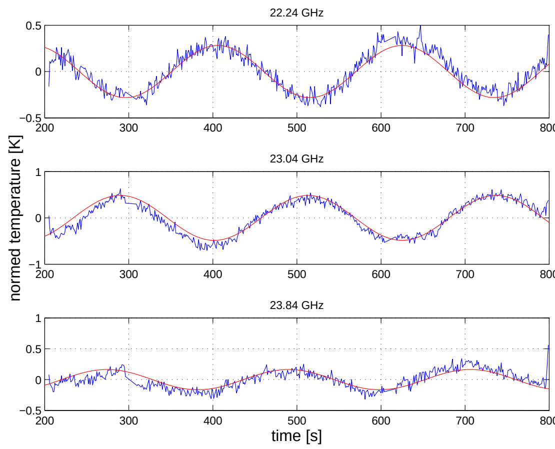

Figure 1. Normalized brightness temperature deviations from the mean over a 10-minute period in Jülich for three HATPRO frequencies (blue) with their respective sine fits (red). The instrument was pointing on the LN_2 target.

To analyze the source of these differences, brightness temperatures were recorded when looking onto the

LN_2 surface for a longer period. With two HATPRO instruments in Leipzig and Jülich (Germany), several measurements have been performed between November 2011 and May 2012. These tests revealed a distinct oscillation pattern for some of the 14 HATPRO frequencies (mainly in the K-Band, but also for the lower V-Band frequencies). Fig. 1 presents an example for brightness temperature observations in Jülich where the osciallating signal is obvious. Note, that the period as well as the amplitude of the oscillations are different!

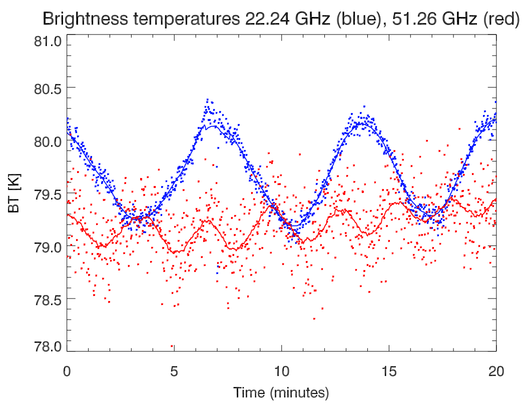

Figure 2. Brightness temperatures 22.24 GHz (blue) and 51.26 GHz (red) for a 20-minute period on 12 December 2011 in Leipzig when pointing onto the LN_2 target. The dots represent the single 1-second observations, the solid lines are a 50-second running mean.

The different oscillation periods can be seen clearly in Fig. 2 where the period for the 22.24 GHz channel is more than double of the 51.26 GHz channel. It becomes obvious that the period depends on the frequency (or wavelength). After evaluation of the oscillation period for all frequencies, a linear relation between wavelength and period was found (see Fig. 3) with a correlation coefficent $r > 0.99$ for both days.

These observations led to the hypothesis that standing waves were forming between the LN_2 surface and the receiver. As the nitrogen was continuously evaporating, the distance to the receiver was increasing and the standing wave was reaching the receiver with a phase difference depending on LN_2 evaporation rate.

For the two days presented in Fig. 3, the periods were different, which can be explained by external meteorological influences. Under extreme conditions the period can vary nearly by a factor of 10: When calibrating under good protection from wind inside a container, as well as covering the instrument with a bed sheet, the period for 22.24 GHz was as high as 20 minutes, whereas when strongly increasing the evaporation rate with a hairdryer, the period was reduced to 3 minutes for the same frequency.

Not only the period, but also the amplitude of the oscillation depends on the frequency. This might be due to the fact that the geometry horn antenna is optimized for a certain wavelength in the center of the both receiver bands.

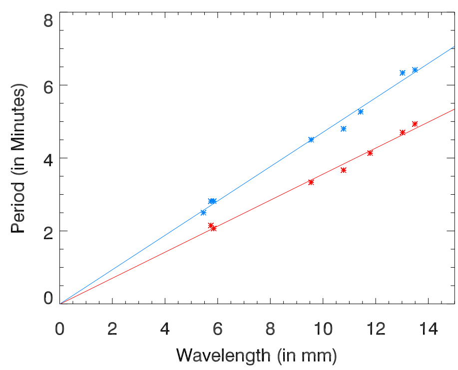

Figure 3. Oscillation period of standing waves when looking on the LN_2 surface as a function of wavelength for two different days, 12 December 2011 (blue) and 19 December 2011 (red). Solid lines represent linear regression for these two days. Correlation coefficient between period and wavelength is > 0.99 for both days.

3.3. Error estimation

With these new findings, the maximum possible error that can be done has to be estimated with an automatic LN_2 calibration. The software algorithm uses a standard integration time on the cold target of 30 seconds. During this time, the standing wave might just be at its lowest or highest value. With an amplitude of the oscillation of up to 0.7 K and a period of 2–20 minutes, the difference between two calibrations might therefore be on the order of 1.5 K. It is not yet completely understood whether the mean or the minimum value represent the brightness temperature value which is assumed in the calibration algorithm. For this reason, the maximum absolute calibration error lies between 0.7 and 1.5 K, respectively.

4. SUMMARY AND OUTLOOK

It has been shown that at the LN_2 calibration of two different HATPRO microwave radiometers standing wave patterns between the LN_2 surface and the receiver occur at some frequencies. The period of these oscillation is frequency dependent, and the amplitude varies significantly between different channels.

In order to come up with this issue, the software of HATPRO will be changed so that a whole standing wave cycle is used for the LN_2 calibration. In a further step, other HATPRO instruments will be evaluated: First results show no oscillation pattern at first generation HATPRO instruments.

ACKNOWLEDGMENTS

We thank all people who were involved in the LN_2 calibrations in Leipzig and Jülich, respectively. Special thanks go to Master students from the University of Leipzig who performed these calibration tests within a practical course.

REFERENCES

[1] Westwater, E., Crewell, S. & Mätzler, C. (2004). A Review of Surface-based Microwave and Millimeter wave Radiometric Remote Sensing of the Troposphere. *Radio Science Bulletin of URSI* **310**, 59–80.

[2] Löhnert, U., Turner, D. D. & Crewell, S. (2009). Ground-based temperature and humidity profiling using spectral infrared and microwave observations. Part 1. Retrieval performance in clear sky conditions. *J. Appl. Meteorol. Clim.* **48**, 1017–1032.

[3] Crewell, S. & Löhnert, U. (2003). Accuracy of cloud liquid water path from ground-based microwave radiometry. Part 2: Sensor accuracy and synergy. *Radio Sci.* **38**, 8041, doi:10.1029/2002RS002634.

[4] Rose, T., Crewell, S., Löhnert, U. & Simmer, C. (2005). A network suitable microwave radiometer for operational monitoring of the cloudy atmosphere. *Atmos. Res.* **75**, 183–200.

[5] Maschwitz, G., Löhnert, U., Crewell, S., Rose, T. & Turner, D. D. (2012). Investigation of Passive Microwave Radiometer Calibration Techniques at 530 hPa. *IEEE Transactions on Geosciences and Remote Sensing* **-**, submitted.